Journal of
Nanoscience and Nanotechnology
Vol. 8, 1–4, 2008

Resistance Switching Characteristics of Zirconium Oxide Containing Gold Nanocrystals for Nonvolatile Memory Applications

Weihua Guan, Shibing Long, Yuan Hu, Qi Liu, Qin Wang, and Ming Liu*

Laboratory of Nano-Fabrication and Novel Devices Integrated Technology, Institute of Microelectronics, Chinese Academy of Sciences, Beijing, 100029, China

Resistance switching characteristics of ZrO_2 films with gold nanocrystals (nc-Au) embedded are investigated for nonvolatile memory applications. The sandwiched structure of top Au electrode/ZrO_2 (with nc-Au embedded)/n^+ Si exhibits two stable resistance states (high-resistance state and low-resistance state). By applying proper voltage bias, resistance switching from one state to the other can be achieved. This resistance switching behavior is reproducible and the ratio between the high and low resistance states can be as high as two orders. A long memory retention time and over 10^2 times DC sweep cycles are demonstrated. The ZrO_2 films employing gold nanocrystals are promising to be used in the nonvolatile memory devices.

Keywords: Resistance Switching, ZrO_2, Nonvolatile Memory, Resistive Random Access Memory (RRAM).

RESEARCH ARTICLE

1. INTRODUCTION

With conventional FLASH memories approaching their scaling limit, a great amount of research efforts have focused their attention on the next generation memory devices. Recently, reversible and reproducible resistance switching phenomena induced by applied external electric field has been extensively studied due to its potential applications in resistive random access memories (RRAM).[1–6] The typical RRAM cell is a capacitor-like structure: a functional material sandwiched between two conductive electrodes. This type of devices can be characterized by two distinct resistance states: OFF state (having high resistance) and ON state (having low resistance). RRAM offers the possibility of high density integration and lower power consumption. The candidate materials for this type of memories include doped perovskite oxide such as $SrZrO_3$ (Ref. [1]) and $SrTiO_3$,[2] ferromagnetic material such as $Pr_{1-x}Ca_xMnO_3$,[3] organic materials[4] and binary transition metal oxides.[5–6] Compared with the other complex materials, binary transition metal oxides (BTMO) such as NiO (Ref [5]) and TiO_2 (Ref. [6]) have the following advantages: simple structure, compatible with the complementary metal-oxide semiconductor (CMOS) technology, and low process temperature. Although a variety of materials have been found to have the resistance switching characteristics, the switching mechanism has not been well understood yet. This may be due to the fact that the performances of these devices depend strongly on the property of the thin films which is not easy to control.

In this study, we propose a novel concept of resistive switching based on gold nanocrystals. The top Au electrode/gold nanocrystals encompassed by ZrO_2/n^+ Si sandwiched structure is fabricated and investigated for nonvolatile memory (NVM) applications for the first time.

2. EXPERIMENTAL DETAILS

After chemically cleaning the heavily doped *n*-type silicon wafer, three sequential layers of ZrO_2/Au/ZrO_2 (with thickness of 25/2/25 nm) are deposited on the substrate via e-beam evaporation. We choose Si wafers as the substrate in this study because it is favorable to incorporate the prepared structure in the standard Si microelectronic technology. The deposition velocity for thin Au wetting layer and two ZrO_2 layers is 0.3 Å/s and 1 Å/s respectively and the chamber pressure is 2.6×10^{-6} Torr. The thickness of each layer is monitored by a quartz crystal oscillator. Post-deposition thermal annealing under several temperatures (700 °C, 800 °C and 900 °C) is carried out in N_2 ambient (3 L/min) for 2 minutes in order to crystallize ZrO_2, passivate the defects in ZrO_2 film and

*Author to whom correspondence should be addressed.

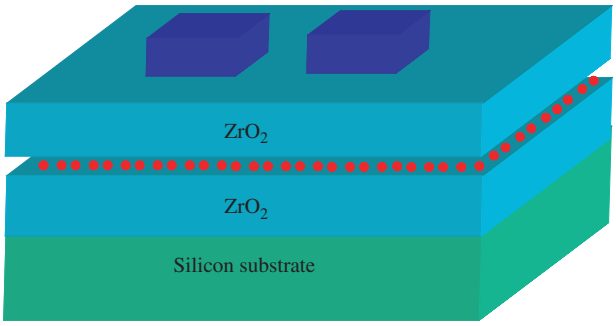

Fig. 1. Schematic structure of fabricated sandwiched structure: top Au electrode/ZrO_2 with Au nanocrystal (nc-Au) embedded/n^+ Si substrate.

induce the formation of gold nanocrystals (nc-Au).[7] After this step, the crystalline profile of ZrO_2 films is characterized by X-ray diffraction (Model M21X, MAC Science Co. Ltd., Japan, Cu Kα, $\lambda = 1.5405$ Å). Finally, 50 nm thick square-shaped Au top electrodes are evaporated and defined by the lift-off process. The resulting sandwiched structure is schematically illustrated in Figure 1, which is quite similar to the structure proposed by Ma et al.[4] However, the material adopted is different (in their case the function layer is AIDCN, an organic material). Control samples without Au nanocrystals embedded in ZrO_2 films are simultaneously fabricated with the same process. The current–voltage (I–V) characteristic of the structure is analyzed by Keithley 4200 Semiconductor Characterization System at room temperature.

3. RESULTS AND DISCUSSION

Figure 2 shows the X-ray diffraction (XRD) patterns of ZrO_2 thin films (without Au layer) annealed at different temperatures. As is shown, for the as-deposited films, there are no obvious diffraction peaks, indicating an amorphous structure. The films are mainly grown in the (−111) orientation at 700 °C annealing, while the crystal growth direction is changed to be (020) and (012) at an annealing temperature of 800 °C and 900 °C. The post-annealing process facilitates the crystalline of the ZrO_2. For the samples with 2 nm Au layer embedded, the same trend of

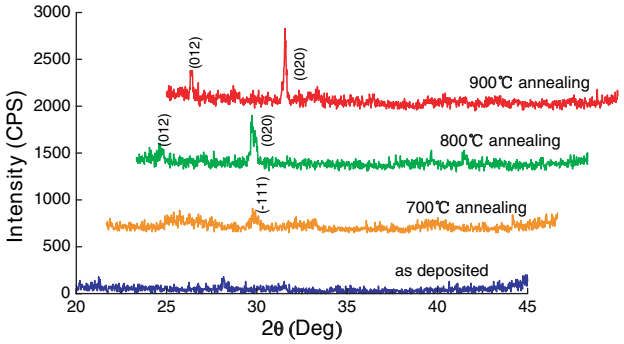

Fig. 2. XRD patterns of zirconium oxide films annealed under various temperature conditions.

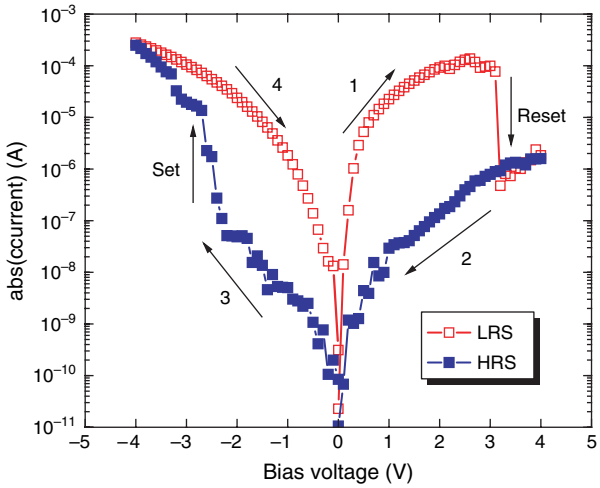

Fig. 3. Typical I–V characteristics for the annealed samples in semi-log scale. The voltage is swept in the direction as: 0 V → 4 V → 0 V → −4 V → 0 V.

X-ray diffraction patterns as Figure 2 is observed. In the electrical measurement, it is found that the electrical performances have strong dependence on the post-annealing process: the as-deposited films exhibit none or unstable resistive switching behaviors while the annealed samples show improved performances. The reasons will be presented in the following discussion.

Figure 3 shows typical current versus voltage (I–V) curves for the annealed samples. As can be seen, a conspicuous hysteresis is observed when the bias is swept back and forth. Resistive switching from the low resistance state (LRS, or ON state) to the high resistance state (HRS, or OFF state) is induced in voltage sweep mode by increasing the voltage up to a value where a sudden decrease in current I is observed. The current of the OFF state increases with increasing the voltage bias in the negative direction and a rapid switching from OFF state to ON state is achieved at a negative bias voltage. At a proper reading voltage (e.g., 0.5 V) the resistance ratio between the two states (HRS/LRS) is nearly two orders. Thus enough margins for sensing the different resistance states are confirmed.

Figure 4 shows the results of DC endurance test for the annealed samples. More than 100 times of Set/Reset cycles without sensing margin deterioration have been demonstrated. Figure 5 shows the current of the HRS and LRS versus the number of switching cycles. As is shown, the current of LRS varied from 3 μA to 90 μA while the current of HRS varied from 6 nA to 58 nA. However, at least 50 times ratio between them can be achieved, large enough to probe the different resistance states.

I–V characteristics of the control sample without nc-Au embedded is also investigated and no or unstable I–V hysteresis is observed (data not shown here). This result confirms the resistive switching effect of the fabricated structure has strong relations with the existence of nc-Au. Although several hypothetical models have been proposed

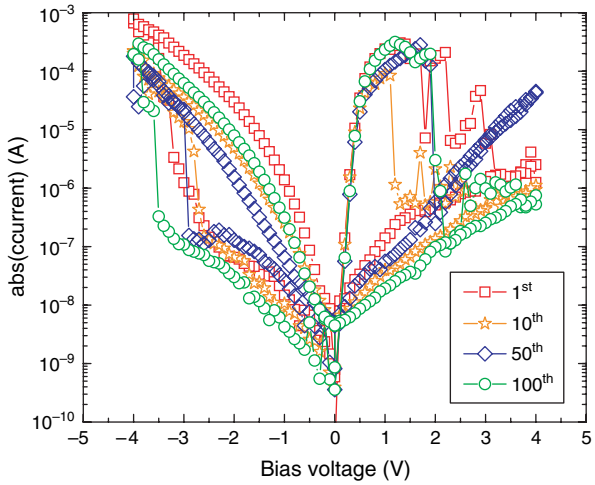

Fig. 4. Endurance performances of the annealedsamples. More than one hundred Set/Reset cycles is demonstrated.

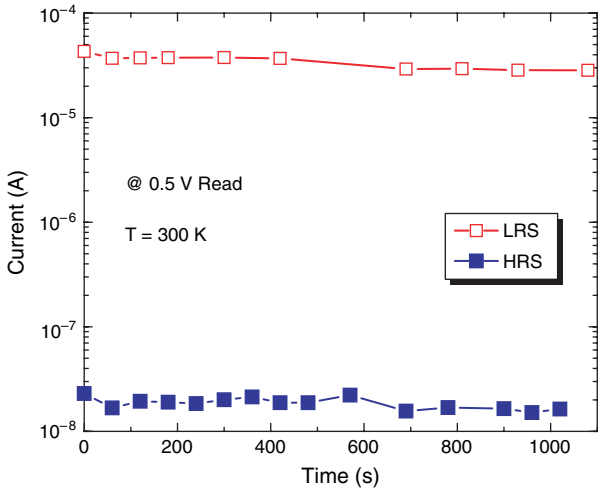

Fig. 6. Long-term stability of cell resistance at room temperature for both the LRS and HRS.

to account for the resistive switching phenomena, for instance, forming and rupture of conductive filaments,[6] space charge limited conduction,[8] trap charging and discharging,[9] the switching mechanism is still not clear yet. According to the electrical characteristics observed, we infer that the resistive switching behavior in the structure is due to the electrons charging and discharging of the nc-Au: When electrons are injected and trapped in nc-Au by applying a positive voltage (e.g., 3 V), an interior electric field is built in the ZrO_2 layer, resulting in the decrease of the conductivity and thus the increase of the resistance, which corresponds to the Reset process. When a negative voltage (e.g., −3 V) is applied, electrons are ejected out of the nc-Au and as a result, the conductivity increases, corresponding to the Set process.

For the samples without nc-Au, as mentioned above, most of them exhibit no resistive switching behavior, some of them, however, show unstable switching phenomenon.

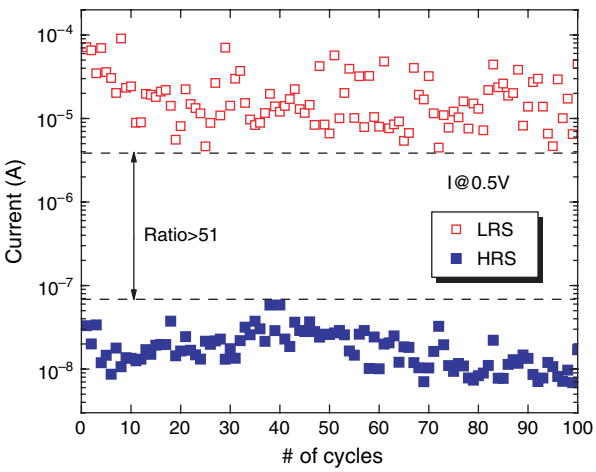

Fig. 5. The current of HRS and LRS versus the number of switching cycles for the fabricated structure at 0.5 V reading voltage. Enough sensing margin is demonstrated.

This may be attributed to the defects and the traps existed in the ZrO_2 films which can be acted as the charging and discharging locations for electrons (similar to the role of nc-Au). These defects and traps, however, are unhomogeneous in the films and thus the resistive switching is not stable. It is also found in the electrical measurement that the resistive switching performances have strong dependence on the post-annealing process: the as-deposited film exhibits unstable resistive switching behaviors while the annealed samples show improved resistive switching performances. This phenomenon can be explained in a similar way: there are a lot of innate defects and traps in the as-deposited samples while the post-annealing process passivates theses defects and traps.

For real non-volatile memory applications, a crucial property of the memory device is its ability to keep information for a long time (retention characteristics). Figure 6 depicts the variation of the current with time for the annealed samples. After a switching bias is applied for a short time, the device is electrically disconnected in either the LRS or the HRS and then periodically recorded the resistance value at an identical reading voltage (0.5 V). The reading of the resistance state is nondestructive, and no electrical power is needed to maintain the resistance in a given state (LRS or HRS). As can be seen, the variation of the LRS and HRS resistance after 10^3 seconds is found to be very little, confirming the nonvolatile nature of the structure.

4. CONCLUSIONS

Zirconium oxide films with nc-Au embedded are deposited by e-beam evaporation to fabricate the top electrode/gold nanocrystals encompassed by ZrO_2/n^+ Si sandwiched structure. This structure possesses the properties of reversible and reproducible resistance switching, nondestructive readout, good endurance performance and

RESEARCH ARTICLE

a long retention time and thus the high potentiality of the fabricated structure for nonvolatile memory applications is confirmed.

Acknowledgments: This work is partly supported by National Basic Research Program of China (973 Program) under Grant No: 2006CB302706 and National Natural Science Foundation of China under Grant No: 90607022, 90401002, and 60506005.

References and Notes

1. A. Beck, J. G. Bednorz, Ch. Gerber, C. Rossel, and D. Widmer, *Appl. Phys. Lett.* 77, 139 (**2000**).
2. W. Xiang, R. Dong, D. Lee, S. Oh, D. Seong, and H. Hwanga, *Appl. Phys. Lett.* 90, 052110 (**2007**).
3. W. W. Zhuang, W. Pan, B. D. Ulrich, J. J. Lee, L. Stecker, A. Burmaster, D. R. Evans, S. T. Hsu, M. Tajiri, A. Shimaoka, K. Inoue, T. Naka, N. Awaya, A. Sakiyama, Y. Wang, S. Q. Liu, N. J. Wu, and A. Ignatiev, *Tech. Dig. IEDM* 193 (**2002**).
4. L. P. Ma, J. Liu, and Y. Yang, *Appl. Phys. Lett.* 80, 2997 (**2002**).
5. K. Kinoshita, T. Tamura, M. Aoki, Y. Sugiyama, and H. Tanaka, *Appl. Phys. Lett.* 89, 103509 (**2006**).
6. B. J. Choi, D. S. Jeong, S. K. Kim, S. Choi, J. H. Oh, C. Rohde, H. J. Kim, C. S. Hwang, K. Szot, R. Waser, B. Reichenberg, and S. Tiedke, *J. Appl. Phys.* 98, 033715 (**2005**).
7. W. Guan, S. Long, M. Liu, Z. Li, Y. Hu, and Q. Liu. *J. Phys. D: Appl. Phys.* 40, 2754 (**2007**).
8. A. Chen, S. Haddad, Y.-C. Wu, T.-N. Fang, Z. Lan, S. Avanzino, S. Pangrle, M. Buynoski, M. Rathor, W. Cai, N. Tripsas, C. Bill, M. VanBuskirk, and M. Taguchi, *Tech. Dig. IEDM* 746 (**2005**).
9. I. G. Baek, M. S. Lee, S. Seo, M. J. Lee, D. H. Seo, D.-S. Suh, J. C. Park, S. O. Park, H. S. Kim, I. K. Yoo, U.-In. Chung, and J. T. Moon, *Tech. Dig. IEDM* 587 (**2004**).

Received: 7 June 2007. Accepted: 29 November 2007.

RESEARCH ARTICLE